

Muted change in Atlantic overturning circulation over some glacial-aged Heinrich events

Jean Lynch-Stieglitz¹, Matthew W. Schmidt², L. Gene Henry^{1,7}, William B. Curry³, Luke C. Skinner⁴, Stefan Mulitza⁵, Rong Zhang⁶, Ping Chang²

¹School of Earth and Atmospheric Sciences, Georgia Institute of Technology, Atlanta, GA, 30307, USA jean@eas.gatech.edu.

²Department of Oceanography, Texas A&M University, College Station, TX, 77843, USA.

³Woods Hole Oceanographic Institution, Woods Hole, MA 02543, USA.

⁴Godwin Laboratory for Palaeoclimate Research, Department of Earth Sciences, University of Cambridge, Downing Street, Cambridge CB2 3EQ, UK.

⁵MARUM—Center for Marine Environmental Sciences, University of Bremen, Leobener Strasse, D-28359 Bremen, Germany.

⁶NOAA/Geophysical Fluid Dynamics Laboratory, Princeton, NJ 08540, USA

⁷Now at Department of Earth and Environmental Sciences and Lamont-Doherty Earth Observatory of Columbia University, Palisades, NY 10964

Contents:

Supplemental Methods: Deep North Atlantic Carbon Isotope Stacks

Supplemental Figure 1. Deep North Atlantic Oxygen Isotope Records

Supplemental Figure 2. Deep North Atlantic Carbon Isotope Records

Supplemental Figure 3. North Atlantic Carbon Isotope Stack

Supplemental Figure 4. Measurements on Individual Foraminifers

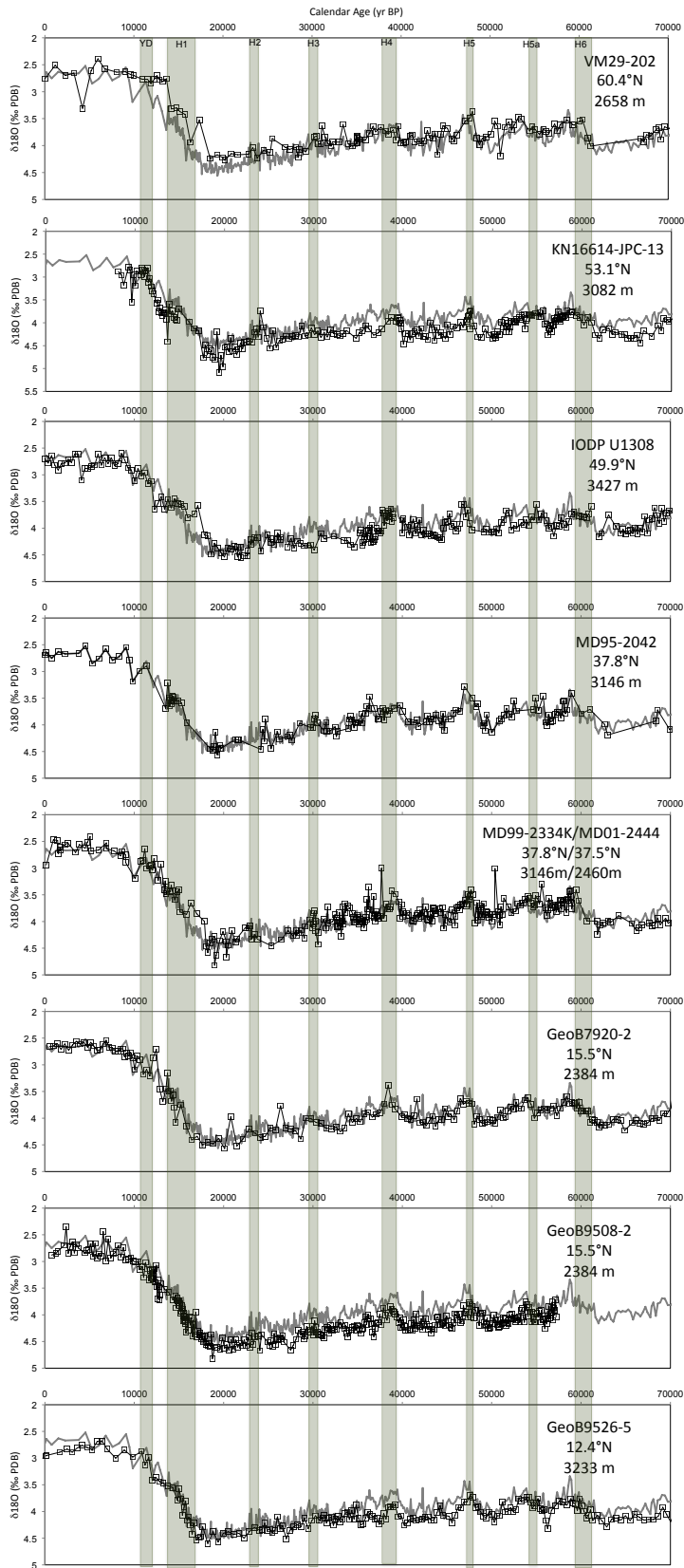
Supplemental Table 1. Age Control Points

Supplemental Table 2. Sediment Core Locations and Sources for Carbon Isotope Stack

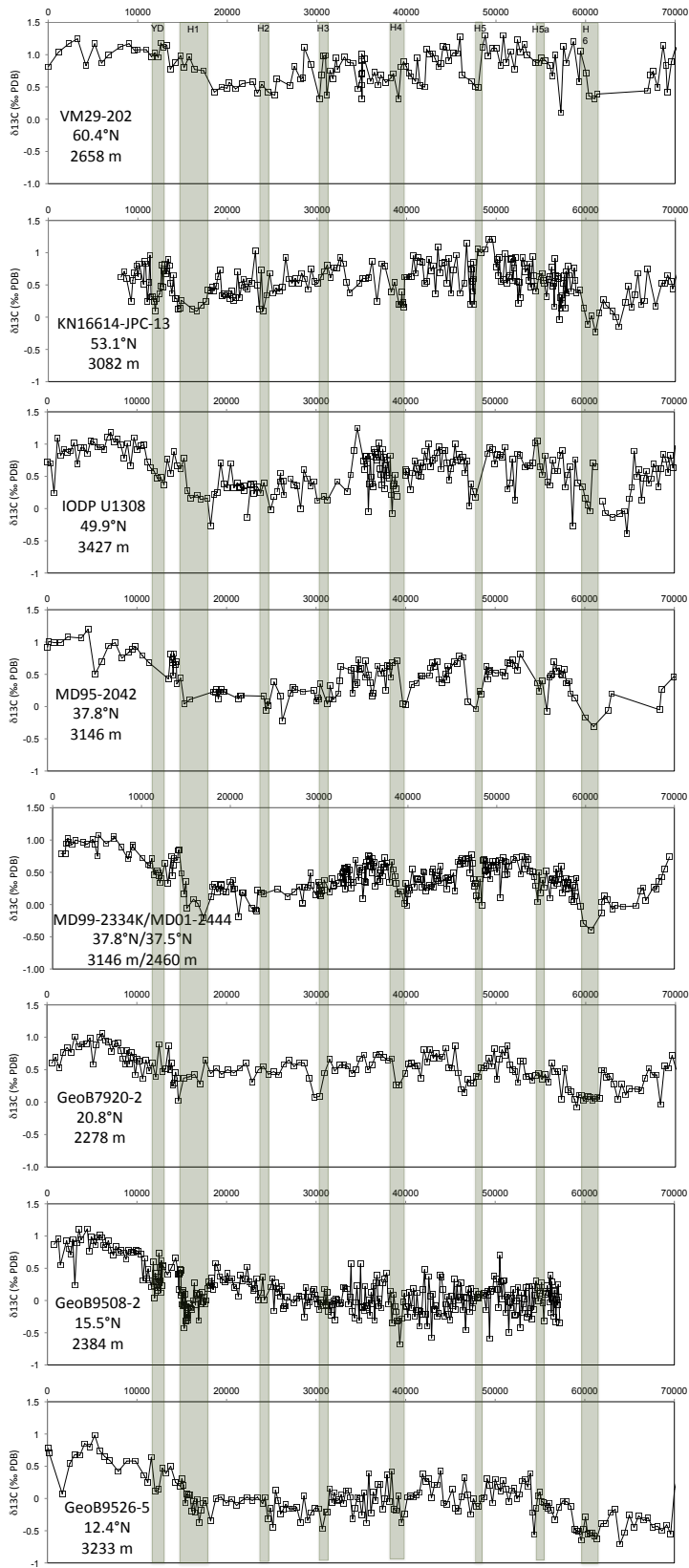
Supplementary References

Supplemental Methods: Deep North Atlantic Carbon Isotope Stacks

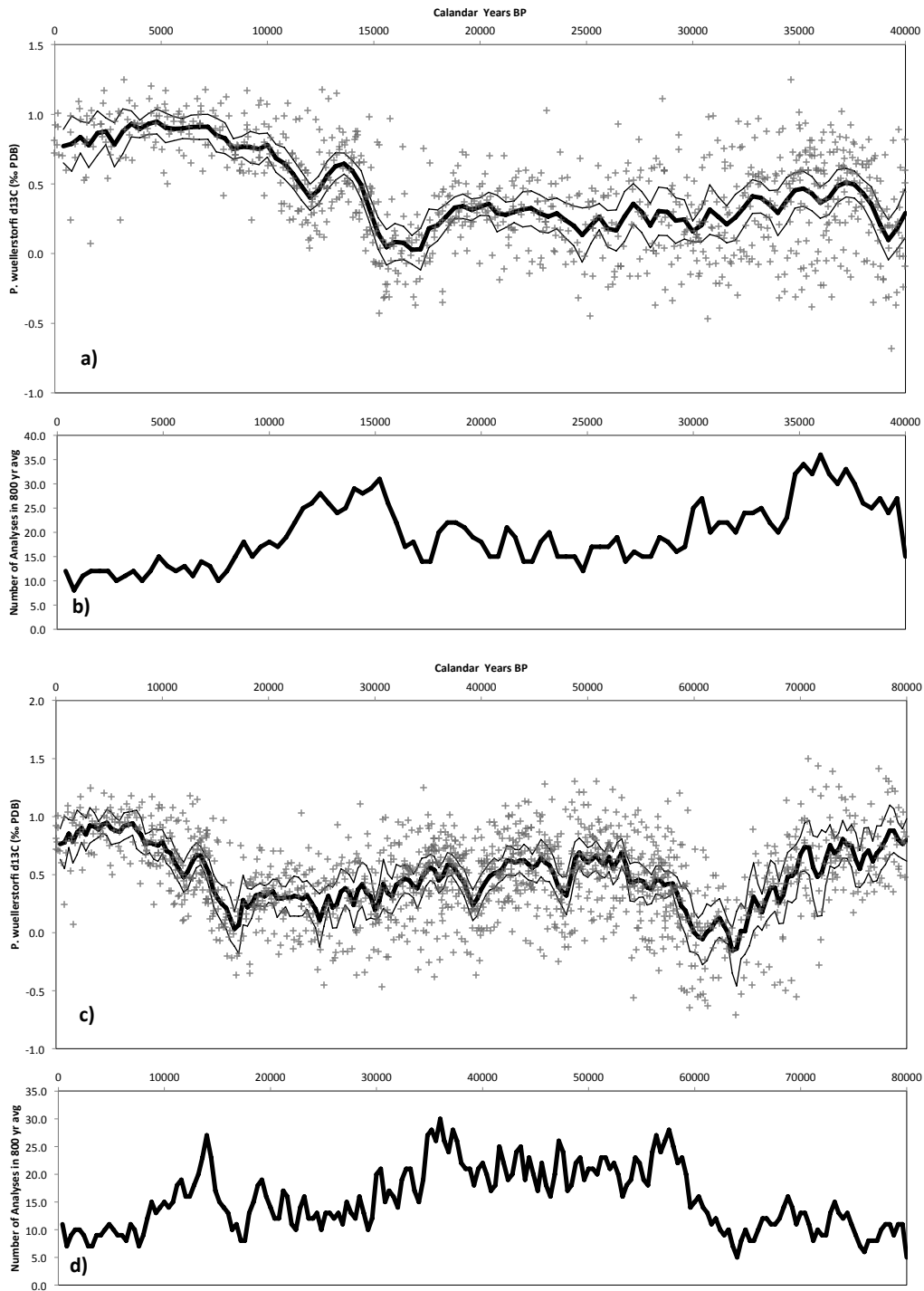
Seven benthic *P. wuellerstorfi* $\delta^{13}\text{C}$ records from the deep North Atlantic were averaged to compute a stacked $\delta^{13}\text{C}$ time series for the last 80 kyr¹⁻⁸. An additional, shorter, record⁹ was used to create an eight record 40 kyr stack (Supplemental Table 2, Supplemental Figures 1-3). All records in this compilation meet or exceed an average time resolution of 500 years and are from greater than 2.2 km depth. All records were placed on a common timescale. For the upper portion of the cores, the age models were constructed using radiocarbon dates converted to calendar age using Calib 6.0 and the MARINE09 calibration data set¹⁰. Below the level for which radiocarbon dates were available, the age models were constrained by correlation of the *P. wuellerstorfi* $\delta^{18}\text{O}$ to the benthic $\delta^{18}\text{O}$ record from MD95-2402 using the modified Greenland ice-core age-scale (SFCP04)¹¹ that has been shown to be broadly consistent with the North Atlantic event stratigraphy implied by the Hulu speleothem record¹². All records except the following two were previously published with time scales constructed in this way. For GeoB7920⁶, subsequently published radiocarbon data¹³ were converted to calendar age and used to constrain the age model above 300 cm depth in the core, and below 300 cm published tie points to the MD95-2042 benthic $\delta^{18}\text{O}$ record were converted to the SFCP04 timescale. For V29-202³ radiocarbon data were converted to calendar age and used to constrain the age model above 300cm and below 300 cm the benthic $\delta^{18}\text{O}$ data was tied to the MD95-2042 benthic $\delta^{18}\text{O}$ record on the SFCP04 timescale.



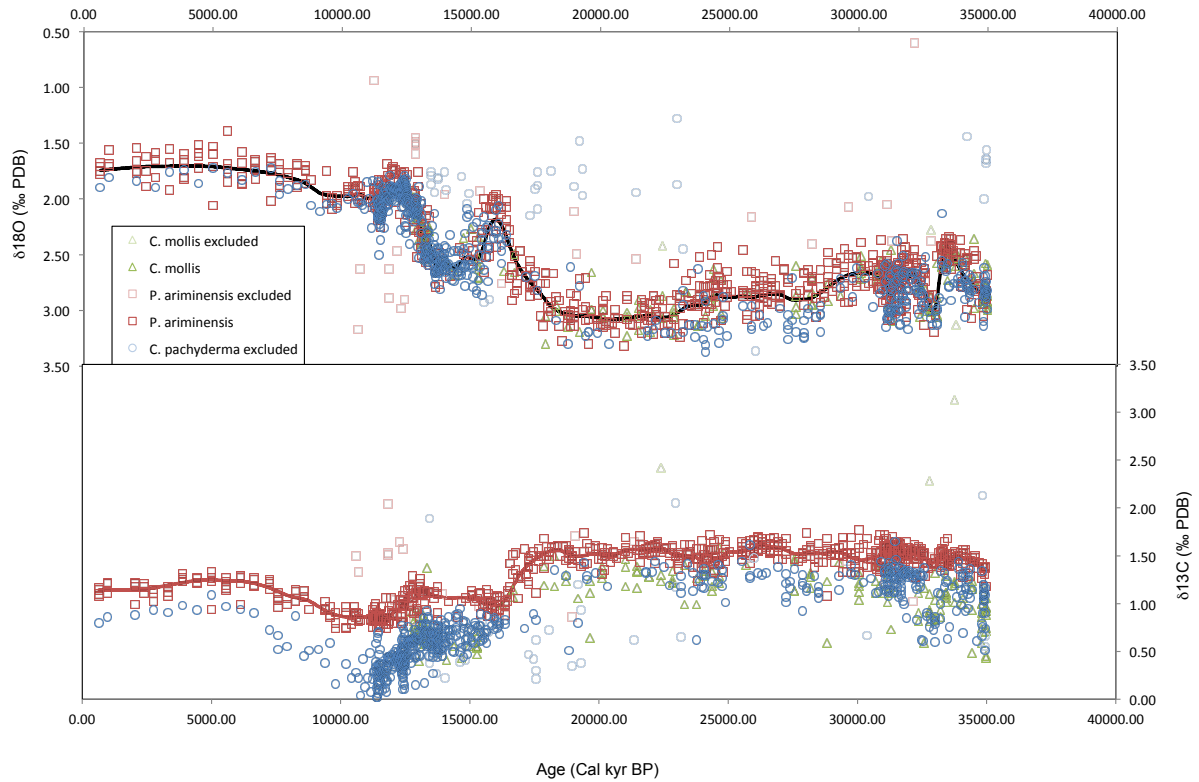
Supplemental Figure 1. Deep North Atlantic Oxygen Isotope Records. High resolution *P. wuellerstorfi* oxygen isotope records from the deep North Atlantic. The locations and sources for each record can be found in Supplemental Table 2. The time scales are constructed as described in the methods section. Grey vertical bars extending through all of the plots indicate the timing of the Younger Dryas and Heinrich stadials¹⁴ For reference, the benthic oxygen isotope record from MD95-2042 on the SFCP04 Age scale¹¹ is also shown in grey in each plot.



Supplemental Figure 2. Deep North Atlantic Carbon Isotope Records. The *P. wuellerstorfi* carbon isotope records from the deep North Atlantic. The locations and sources for each record can be found in Supplemental Table 2. The time scales are constructed as described in the methods section. Grey vertical bars extending through all of the plots indicate the timing of the Younger Dryas and Heinrich stadials¹⁴.

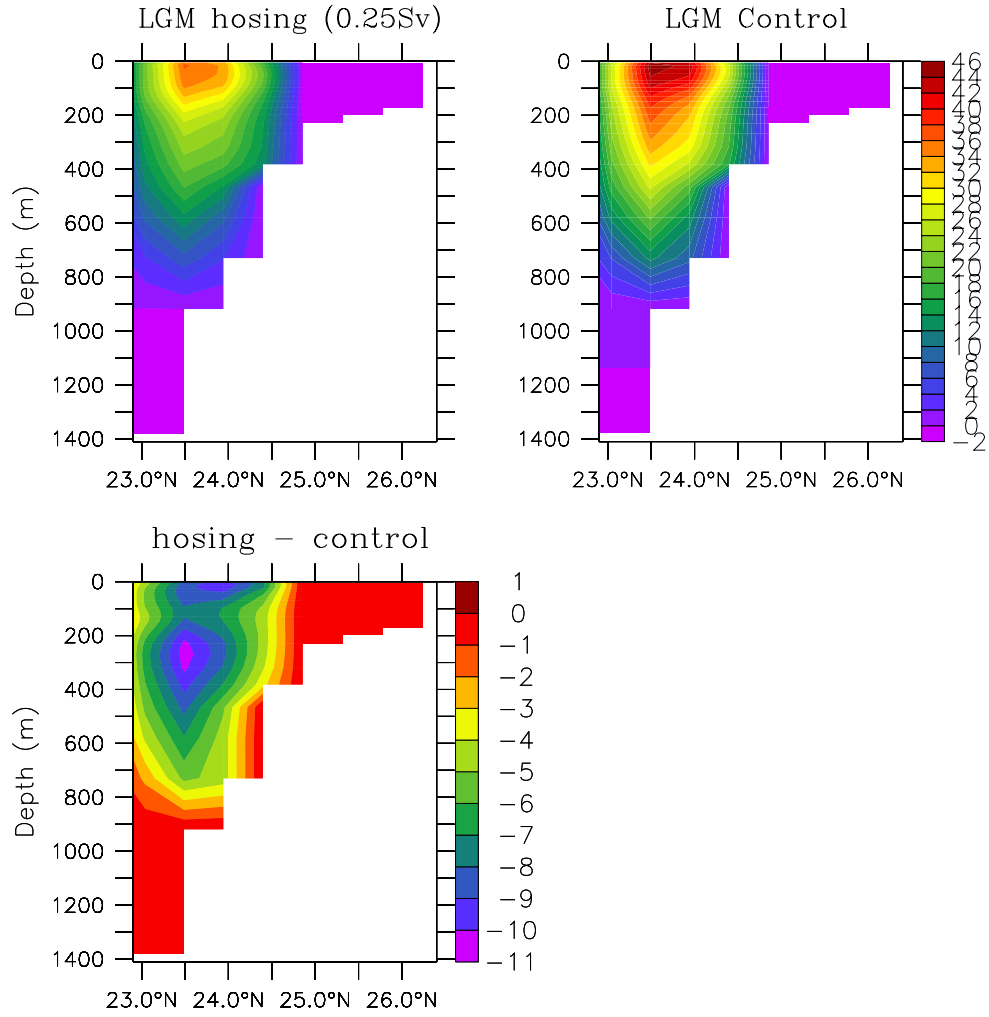


Supplemental Figure 3. North Atlantic Carbon Isotope Stack. For panels (a) and (c) the light crosses show the individual data points contributing to the 40 kyr and 80 kyr averages, respectively. The solid heavy lines are the average (800 year window) and lighter lines are ± 2 standard error of the 800 year averages. Panels (b) and (d) show the total number of analyses contributing to each 800 year average for the 40 kyr and 80 kyr averages, respectively.

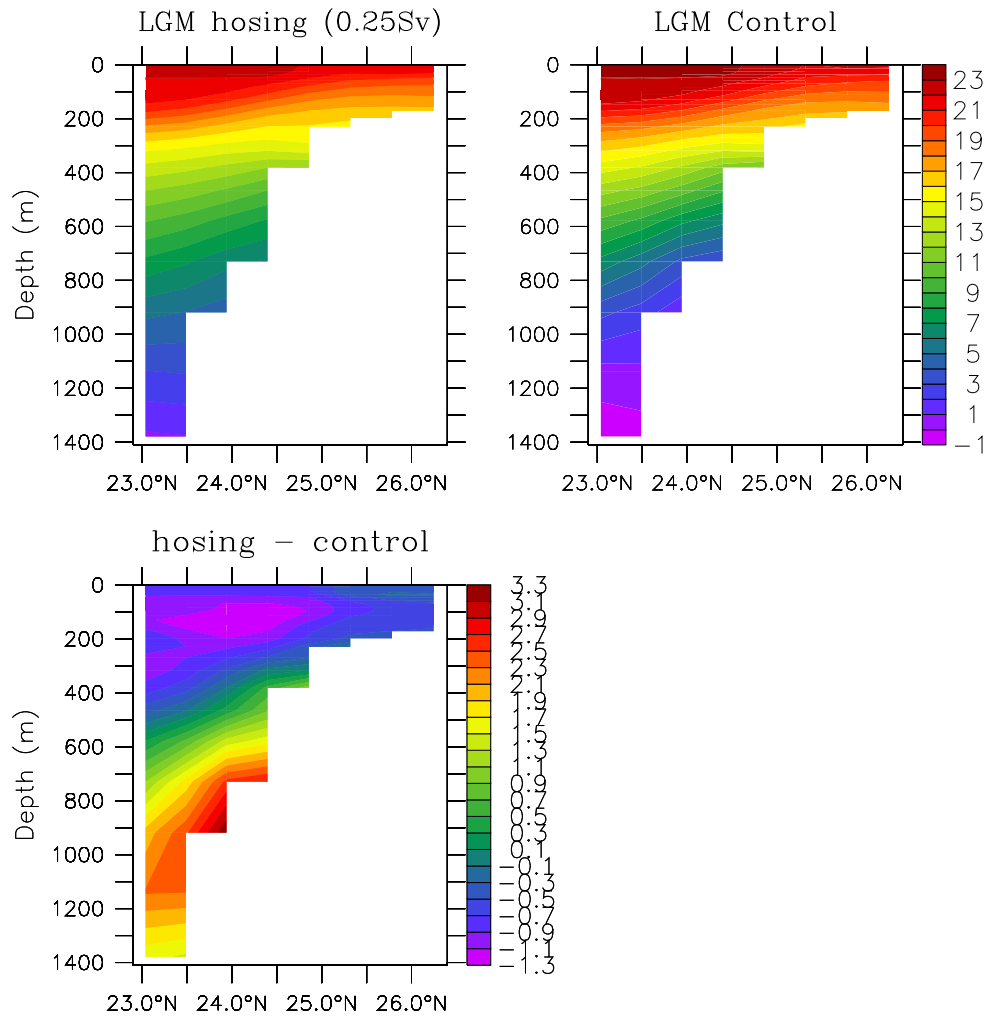


Supplemental Figure 4. Measurements on Individual Foraminifera a) $\delta^{18}\text{O}$ for individual measurements contributing to the average values at each depth shown in Figure 2. The 4% of the measurements not contributing to the averages because they have been flagged as having a distance from the robust loess smooth of the data (black line) greater than 2 standard deviations from the mean are indicated in a lighter shade. b) $\delta^{13}\text{C}$ for individual measurements. Only the data from *P. ariminensis* contribute to the depth average values shown in Figures 2 and 4.

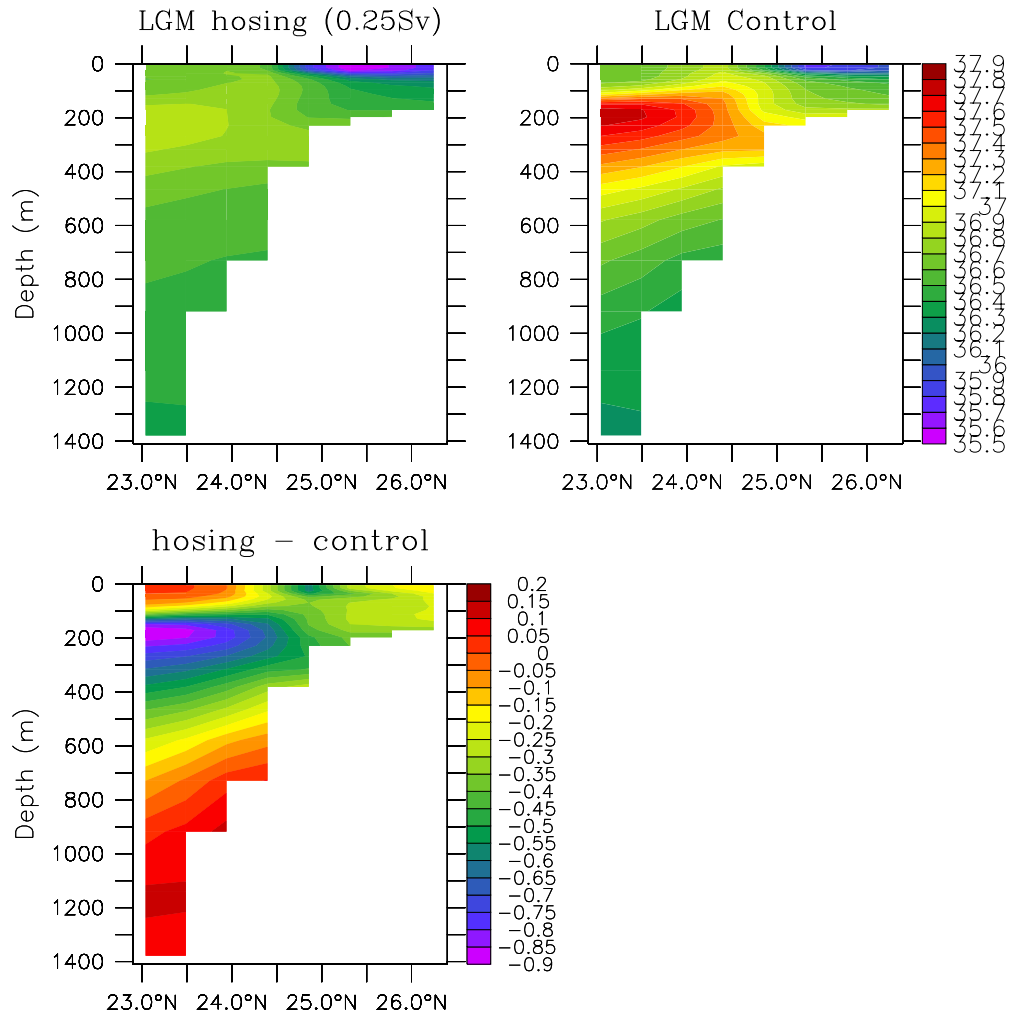
a)



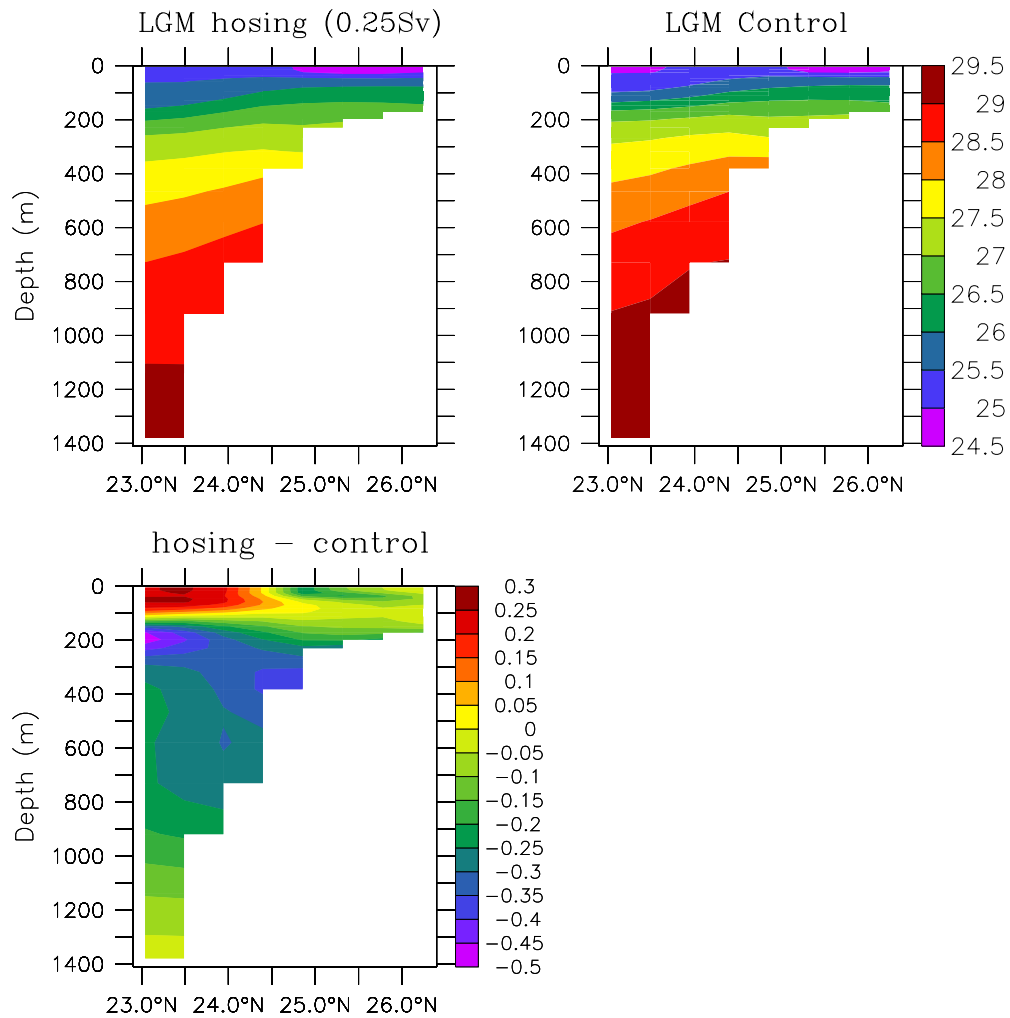
b)



c)



d)



Supplemental Figure 5. Florida Straits Sections along 83°W in CCSM3. For each panel the values for the LGM control run, the last 30 years of the water hosing experiment (0.25 Sv) and the anomaly (hosing – control) are shown¹⁵. a) velocity (cm s^{-1}) b) Temperature ($^{\circ}\text{C}$) c) Salinity (psu) d) Sigma-theta.

| Core | Depth in core | species | ¹⁴ C age | error | Calendar Age | Source | |
|----------------|----------------|--------------------------------|---------------------|-------|------------------|------------------------------|------------------------------|
| KNR166-2 26JPC | 0.75 | <i>G. sacculifer</i> | 1070 | 70 | 634 | Lynch-Stieglitz et al., 2011 | |
| | 48.25 | <i>G. sacculifer</i> | 2990 | 30 | 2760 | Lynch-Stieglitz et al., 2011 | |
| | 112.25 | <i>G. sacculifer</i> | 6720 | 40 | 7251 | Lynch-Stieglitz et al., 2011 | |
| | 144.25 | <i>G. sacculifer</i> | 8100 | 80 | 8576 | Lynch-Stieglitz et al., 2011 | |
| | 216.25 | <i>G. sacculifer</i> | 9550 | 40 | 10418 | Lynch-Stieglitz et al., 2011 | |
| | 280.25 | <i>G. sacculifer, G. ruber</i> | 10100 | 45 | 11130 | Lynch-Stieglitz et al., 2011 | |
| | 344.25 | <i>G. sacculifer</i> | 10000 | 110 | 10944* | Lynch-Stieglitz et al., 2011 | |
| | 356.25 | <i>G. sacculifer</i> | 11750 | 95 | 13225* | Lynch-Stieglitz et al., 2011 | |
| | 364.25 | <i>G. sacculifer, G. ruber</i> | 10600 | 70 | 11872* | Lynch-Stieglitz et al., 2011 | |
| | 374.25 | <i>G. sacculifer</i> | 10500 | 50 | 11656* | Lynch-Stieglitz et al., 2011 | |
| | 392.25 | <i>G. ruber</i> | 10850 | 65 | 12342* | Lynch-Stieglitz et al., 2011 | |
| | 408.25 | <i>G. sacculifer, G. ruber</i> | 10300 | 60 | 11285* | Lynch-Stieglitz et al., 2011 | |
| | 442.25 | <i>G. sacculifer, G. ruber</i> | 10700 | 65 | 12077 | Lynch-Stieglitz et al., 2011 | |
| | 464.25 | <i>G. sacculifer, G. ruber</i> | 10800 | 55 | 12251 | Lynch-Stieglitz et al., 2011 | |
| | 544.25 | <i>G. sacculifer, G. ruber</i> | 11000 | 65 | 12515 | Lynch-Stieglitz et al., 2011 | |
| | 592.25 | <i>G. ruber</i> | 11400 | 65 | 12866 | Lynch-Stieglitz et al., 2011 | |
| | 606.25 | <i>G. sacculifer</i> | 11600 | 35 | 13106 | Lynch-Stieglitz et al., 2011 | |
| | 648.25 | <i>G. sacculifer</i> | 12350 | 200 | 13807 | Lynch-Stieglitz et al., 2011 | |
| | 704.25 | <i>G. ruber</i> | 13500 | 55 | 15857 | Lynch-Stieglitz et al., 2011 | |
| | 752.25 | <i>G. ruber</i> | 15550 | 70 | 18271 | Lynch-Stieglitz et al., 2011 | |
| | 848.25 | <i>G. ruber</i> | 20300 | 120 | 23760 | Lynch-Stieglitz et al., 2011 | |
| | 878.25 | <i>G. sacculifer, G. ruber</i> | 21300 | 95 | 24896 | this study | |
| | 952.25 | <i>G. ruber</i> | 26300 | 130 | 30693 | Lynch-Stieglitz et al., 2011 | |
| | 1014.25 | <i>G. ruber</i> | 28200 | 180 | 31890 | Lynch-Stieglitz et al., 2011 | |
| | 1032.25 | <i>G. ruber</i> | 28200 | 590 | 32160* | Lynch-Stieglitz et al., 2011 | |
| | 1074.25 | <i>G. ruber</i> | 29300 | 380 | 33482 | Lynch-Stieglitz et al., 2011 | |
| | 1088.25 | <i>G. sacculifer, G. ruber</i> | 31300 | 200 | 35398* | this study | |
| | 1104.25 | <i>G. sacculifer, G. ruber</i> | 30600 | 170 | 34800 | this study | |
| | 1118.25 | <i>G. sacculifer</i> | 30900 | 220 | 34958 | Lynch-Stieglitz et al., 2011 | |
| | KNR166-2 73GGC | 0.25 | mixed planktonics | 650 | 35 | 297 | Lynch-Stieglitz et al., 2011 |
| | | 28.25 | mixed planktonics | 2670 | 30 | 2357 | Lynch-Stieglitz et al., 2011 |
| 48.25 | | <i>G. sacculifer</i> | 3510 | 30 | 3394 | Lynch-Stieglitz et al., 2011 | |
| 96.25 | | <i>G. sacculifer</i> | 5040 | 40 | 5388 | Lynch-Stieglitz et al., 2011 | |
| 152.25 | | <i>G. sacculifer</i> | 6580 | 40 | 7102 | Lynch-Stieglitz et al., 2011 | |
| 168.25 | | <i>G. sacculifer</i> | 6890 | 45 | 7404 | Lynch-Stieglitz et al., 2011 | |
| 196.25 | | <i>G. sacculifer</i> | 9080 | 50 | 9805 | Lynch-Stieglitz et al., 2011 | |
| 212.25 | | <i>G. sacculifer</i> | 10550 | 55 | 11782 | Lynch-Stieglitz et al., 2011 | |
| 224.25 | | <i>G. sacculifer</i> | 12150 | 70 | 13592 | Lynch-Stieglitz et al., 2011 | |
| 232.25 | | <i>G. sacculifer</i> | 18300 | 90 | 21372 | Lynch-Stieglitz et al., 2011 | |
| 240.25 | | <i>G. ruber</i> | 21100 | 95 | 24691 | this study | |
| 248.25 | | <i>G. sacculifer</i> | 22900 | 130 | 27255 | Lynch-Stieglitz et al., 2011 | |
| 266.25 | | <i>G. sacculifer</i> | 29300 | 140 | 33435 | this study | |
| 280.25 | | <i>G. sacculifer</i> | 31000 | 190 | 35019 | Lynch-Stieglitz et al., 2011 | |
| 296.25 | | <i>G. sacculifer</i> | 36800 | 350 | 41474 | Lynch-Stieglitz et al., 2011 | |
| 356.25 | | | | | 63000 | MIS 3/4 boundary | |
| 372.25 | | | | 73000 | MIS 4/5 boundary | | |

Radiocarbon dates calibrated using Calib 6.0 and Marine09 curve

*Not used in age model

Supplemental Table 1. Age Control Points

| Core | Longitude | | | Latitude | | | Depth (m) | Reference |
|-----------------|-----------|----|---|----------|----|---|-----------|--|
| GeoB9508-5 | 17 ° | 57 | W | 15 ° | 30 | N | 2384 | Mulitza et al., (2008) |
| MD99-2334K | 10 ° | 10 | W | 37 ° | 48 | N | 3146 | Skinner et al (2007) |
| MD01-2444 | 10 ° | 8 | W | 37 ° | 33 | N | 2460 | Skinner et al (2007) |
| IODP U1308 | 24 ° | 14 | W | 49 ° | 53 | N | 3883 | Hodell et al. (2008) |
| VM29-202 | 20 ° | 58 | W | 60 ° | 23 | N | 2658 | Oppo and Lehman (1995) |
| KN166-14-JPC-13 | 33 ° | 32 | W | 53 ° | 3 | N | 3082 | Hodell et al. (2010) |
| MD95-2042 | 10 ° | 10 | W | 37 ° | 48 | N | 3146 | Shackleton et al. (2000) |
| GeoB7920-2 | 18 ° | 35 | W | 20 ° | 45 | N | 2278 | Tjallingi et al. (2008) |
| GeoB9526-5 | 18 ° | 3 | W | 12 ° | 26 | N | 3233 | Zarriess and Mackensen (2011), Zarriess (2010) |

Supplemental Table 2. Sediment Core Locations and Sources for Carbon Isotope Stack.

Supplementary References

- 1 Hodell, D. A., Channell, J. E. T., Curtis, J. H., Romero, O. E. & Rohl, U. Onset of "Hudson Strait" Heinrich events in the eastern North Atlantic at the end of the middle Pleistocene transition (similar to 640 ka)? *Paleoceanography* **23**, doi:10.1029/2008PA001591 (2008).
- 2 Hodell, D. A., Evans, H. F., Channell, J. E. T. & Curtis, J. H. Phase relationships of North Atlantic ice-rafted debris and surface-deep climate proxies during the last glacial period. *Quaternary Science Reviews* **29**, 3875-3886, doi:10.1016/J.Quascirev.2010.09.006 (2010).
- 3 Oppo, D. W. & Lehman, S. J. Suborbital Timescale Variability of North-Atlantic Deep-Water During the Past 200,000 Years. *Paleoceanography* **10**, 901-910 (1995).
- 4 Shackleton, N. J., Hall, M. A. & Vincent, E. Phase relationships between millennial-scale events 64,000-24,000 years ago. *Paleoceanography* **15**, 565-569 (2000).
- 5 Skinner, L. C., Elderfield, H. & Hall, M. in *Ocean Circulation: Mechanisms and Impacts Geophysical Monograph Series* (eds A. Schmittner, J. Chiang, & S. Hemming) 197-208 (American Geophysical Union, 2007).
- 6 Tjallingii, R. *et al.* Coherent high- and low-latitude control of the northwest African hydrological balance. *Nature Geoscience* **1**, 670-675, doi:Doi 10.1038/Ngeo289 (2008).
- 7 Zariess, M. & Mackensen, A. Testing the impact of seasonal phytodetritus deposition on delta(13)C of epibenthic foraminifer *Cibicidoides wuellerstorfi*: A 31,000 year high-resolution record from the northwest African continental slope. *Paleoceanography* **26**, doi:Artn Pa2202 Doi 10.1029/2010pa001944 (2011).
- 8 Zariess, M. *Primary Productivity and Ocean Circulation Changes on orbital and millennial Timescales off Northwest Africa during the Last Glacial/Interglacial Cycle: Evidence from benthic foraminiferal Assemblages, stable carbon and oxygen isotopes and Mg/Ca Paleothermometry* Ph.D. thesis, Universitat Bremen, (2010).
- 9 Mulitza, S. *et al.* Sahel megadroughts triggered by glacial slowdowns of Atlantic meridional overturning. *Paleoceanography* **23**, PA4206, doi:Doi 10.1029/2008pa001637 (2008).
- 10 Reimer, P. J. *et al.* Intcal09 and Marine09 Radiocarbon Age Calibration Curves, 0-50,000 Years Cal Bp. *Radiocarbon* **51**, 1111-1150 (2009).
- 11 Shackleton, N. J., Fairbanks, R. G., Chiu, T. C. & Parrenin, F. Absolute calibration of the Greenland time scale: implications for Antarctic time scales and for Delta C-14. *Quaternary Science Reviews* **23**, 1513-1522, doi:Doi 10.1016/J.Quascirev.2004.03.006 (2004).
- 12 Skinner, L. C. Revisiting the absolute calibration of the Greenland ice-core age-scales. *Clim Past* **4**, 295-302 (2008).
- 13 Collins, J. A. *et al.* Interhemispheric symmetry of the tropical African rainbelt over the past 23,000 years. *Nature Geoscience* **4**, 42-45, doi:Doi 10.1038/Ngeo1039 (2011).

- 14 Wang, Y. J. *et al.* A high-resolution absolute-dated Late Pleistocene monsoon record from Hulu Cave, China. *Science* **294**, 2345-2348 (2001).
- 15 Schmidt, M. W. *et al.* Impact of abrupt deglacial climate change on tropical Atlantic subsurface temperatures. *Proceedings of the National Academy of Sciences of the United States of America* **109**, 14348-14352, doi:Doi 10.1073/Pnas.1207806109 (2012).